Sea-ice microbial community succession and the potential role of parasitoids in the maintenance of diversity

Kyle B. Dilliplaine[1]*, Laura M. Whitmore[1,2], Ana Aguilar-Islas[1], Channing Bolt[1,3], Kenneth Dumack[4], Meibing Jin[2], Mette Kaufman[2], Marc Oggier[2], Gwenn M. M. Hennon[1]

[1]College of Fisheries and Ocean Sciences, University of Alaska Fairbanks, Fairbanks, AK, USA
[2]International Arctic Research Center, University of Alaska Fairbanks, Fairbanks, AK, USA
[3]Naval Information Warfare Center, Pacific, San Diego, CA, USA
[4]Aquatic Ecosystem Analyses, Institute for Integrated Natural Sciences, University of Koblenz, Koblenz, Germany

***Corresponding author:** kbdilliplaine@alaska.edu

Email addresses: lmwhitmore@alaska.edu; amaguilarislas@alaska.edu; channing.e.bolt2.civ@us.navy.mil; kenneth.dumack@uni-koblenz.de; mjin@alaska.edu; mrkaufman@alaska.edu; moggier@alaska.edu; gmhennon@alaska.edu

Acknowledgements: The authors thank the Ukpeaġvik Iñupiat Corporation Science (UICS) for their logistical support in Utqiaġvik during field work. We thank Hajo Eicken and Rob Rember who were instrumental to securing funding and planning the field campaign and Anika Pinzer for teaching satellite imagery retrieval and map making skills. This project was supported by research grants funded through the National Science Foundation (NSF) OPP-1735862 (AAI) and OCE-1937715 (GMH) and the Coastal Marine Institute M20AC10007 (GMH), a joint institute between the Bureau of Ocean Energy Management (BOEM) and the University of Alaska Fairbanks. Kenneth Dumack was supported by the German Research Foundation (DFG) with the grant number 555596351. Micrographs were captured at the UAF Molecular Imaging Facility, NIGMS P20GM130443.

Conflict of Interest: The authors declare no conflict of interest.

Data Availability: Biogeochemical data are available through the Arctic Data Center, doi:10.18739/A21J9793S (Whitmore et al., 2024), and DNA sequencing data are available through NCBI's SRA under BioProject PRJNA1108783. Taxonomically annotated Raw read counts are available as a supplementary dataset Supplementary Information (Table S1 & S2). Data processing and analysis R scripts are publicly available on GitHub at https://github.com/kbdilliplaine/2021-Utqiagvik-time-series.git.

Author Contributions (CRediT):
Conceptualization: KBD and GMH contributed to the conceptualization of overarching research goals and aims.
Data curation: LW, KBD and MO contributed to data curation.
Formal analysis: KBD and LW contributed to formal analysis.
Funding acquisition: AAI acquired funding to support the project leading to this publication. GMH acquired funding to support sample processing, labor, and publication costs.
Investigation: LW, CB, MK and MO conducted field work and processed samples for physical and chemical properties. KBD processed samples for molecular analysis.
Methodology: AAI, MO, LW and KBD contributed to methodological development.

Project administration: GMH and AAI managed different aspects of this project and its execution.
Resources: AAI, MK and GMH contributed resources necessary for the completion of this study.
Visualization: KBD was responsible for the creation of all visual components of this manuscript.
Writing – original draft: KBD was responsible for the creation of the initial draft.
Writing – review & editing: GMH, LW, KD, MJ and AAI provided substantial critical review and commentary of this manuscript.

Abstract

Sea ice is a crucial, yet declining, habitat in high latitude ecosystems. Here we present a high-temporal resolution amplicon sequence data set collected during the vernal ice-algal bloom near Utqiaġvik, Alaska in 2021 to study sea-ice microbial dynamics. The ice-algal bloom peaked on May 8th, reaching 46.6 mg chlorophyll *a* m^{-2}, and thereafter became limited by nitrate availability. A massive bloom of the oil-degrading bacterium, *Oleispira* (>80% relative abundance), coincided with the algal bloom raising questions about hydrocarbon exposure. The sea-ice algal bloom was dominated by diatoms, particularly *Nitzschia spp.*, and transitioned into a flagellate dominated post-bloom community which aligned with melt-associated irradiance increase and nutrient flushing. We explored the relationship between putative parasitoids, Chytridiomycetes, Thecofilosea (Cercozoa), Oomycetes, Syndiniales (Dinoflagellata), and Labyrinthulomycetes (Bigyra), and potential microalgal hosts. Chytrids peaked periodically suggesting synchronized infections and *Cryothecomonas* (Thecofilosea) was observed parasitizing *Nitzschia spp.* for the first time in Arctic sea ice. Co-occurrence analysis suggested that diatoms, especially *Nitzschia*, were the primary hosts of Arctic parasitoids, and that top-down parasitoid control may dramatically alter community composition over short timescales, such as days. These results provide important insights into the drivers of vernal bloom timing and maintenance of microalgal diversity in sea ice.

Keywords: sea-ice microalgae, parasitoids, *Oleispira*, *Cryothecomonas*, chytrids, landfast sea ice, Utqiaġvik, AK

1. Introduction

Climate change is rapidly impacting the Arctic sea-ice system by shifting the timing of freezeup and melt (Walsh et al., 2022), precipitation patterns (Bintanja and Selten, 2014; Webster et al., 2014), and ice extent and thickness (Stroeve and Notz, 2018; Babb et al., 2022). Sea-ice associated (sympagic) microalgae contribute substantially to Arctic primary production, although estimates vary from 2-10% from modeling studies (Dupont, 2012; Mortenson et al., 2020) to up to 57% from in situ measurements (Gosselin et al., 1997; Gradinger, 2009). Ice-algal production is primarily controlled by the availability of light, which is determined by ice and snow thickness (Mcdonald et al., 2015; Veyssière et al., 2022), and inorganic nutrients supplied via underlying water (Cota et al., 1987; Cota and Smith, 1991). Irradiance levels likely contribute to species-specific succession and community composition due to differing photophysiology (Croteau et al., 2022). For example, centric diatoms (such as *Thalassiosira* spp.*),* dinoflagellates, and certain pennate diatoms (such as *Navicula* spp.), increase with greater light availability while other pennate diatoms like *Nitzschia frigida* decline (Duncan et al., 2024).

Nitrogen is generally the limiting nutrient throughout most of the Arctic (Rózańska et al., 2009; Pineault et al., 2013), though silicic acid, which is required by diatoms, has been found to be limiting regionally (Gosselin and Legendre, 1990; Smith et al., 1990). Nutrient availability can influence microalgal community structure based on the resource utilization traits and stoichiometric requirements of different algal taxa (Litchman, de Tezanos Pinto, et al., 2015; Litchman, Edwards, et al., 2015). Sea ice melt processes release dense algal material which may be grazed by plankton (Juul-Pedersen et al., 2008), sink rapidly to the seafloor as aggregates (Ambrose et al., 2005; Boetius et al., 2013), or seed a successive phytoplankton bloom (Garrison et al., 1987; Lizotte, 2001; Yan et al., 2020). Post-bloom communities have been observed to shift toward heterotrophic protists and dinoflagellates, in association with lower salinity and high irradiance from ice melt (von Quillfeldt et al., 2003; Rózańska et al., 2009). While much is known about bottom-up environmental control of sympagic microbial communities, top-down biological pressures may also affect community composition and are less well-understood.

The study of parasites has been limited to small and focused investigations in sea ice. While fungi such as chytrids (Hassett and Gradinger, 2016), and a newly discovered thraustochytrid (Labyrinthulomycetes), infect sea-ice algae (Hassett, 2020), Arctic *Cryothecomonas* spp. have thus far been observed only as grazers (Thaler and Lovejoy, 2012). In contrast to parasites, parasitoids ultimately kill their host after infection (Skovgaard, 2014). Parasitoids are capable of terminating phytoplankton blooms and altering species succession (Tillmann et al., 1999; Chambouvet et al., 2008). Despite their potential ecological importance, marine parasitoids are understudied due to ambiguous morphologies that make identification difficult (Käse et al., 2021), though molecular surveys suggest high undescribed diversity (Thaler and Lovejoy, 2012; B. T. Hassett et al., 2019). Identifying potential parasitoid-host interactions is required to better understand bloom dynamics and biogeochemical cycles in sea ice where parasitoid infections of microalgae have the potential to modulate the transfer of carbon between trophic levels (Amundsen et al., 2009).

Despite the importance of sympagic microbes to the Arctic ecosystem, basic information regarding microbial community structure, dynamics, and microalgal bloom phenology is spatiotemporally limited along the coastal US Arctic. We conducted a high-resolution time series (2.5 months, sampled every few days) to determine the timing, magnitude, and yield-limiting

factor of the ice-algal bloom at Utqiaġvik, Alaska, formerly known as Barrow. We examined the prokaryotic and unicellular eukaryotic community composition and dynamics over the spring microalgal bloom using 16S and 18S rRNA amplicon sequencing, and leveraged these data to identify putative parasitoid-host relationships within the sympagic community.

2. Methods

2.1. *Study site and ice sampling*

Field collections were conducted near Utqiaġvik, Alaska (71.375 N, 156.537 W) between April 21 and June 11, 2021 (day of year 111 — 162), on a large level pan of landfast sea ice, measuring ~11 km^2 (Fig. S1). Additional site information and details for methodology is provided in the Supporting Information: Appendix 1. Sea ice cores were collected from a ~900 m^2 area, with each sampling event constrained to 1 m^2 in an attempt to reduce spatial heterogeneity of ice core properties. Ice core samples were collected three times per week, as weather permitted, and measurements of temperature, salinity, density, nutrients, chlorophyll *a* (chl *a*), and samples for DNA were collected (see Supporting Information: Appendix 1 for more details). Cores were retrieved using a 9-cm inner diameter Kovacs ice corer. Incident and under-ice photosynthetically active radiation (PAR; 400-700 nm) photon flux densities were measured adjacent to the sampling area using a LI-COR LI-1400 data logger with planar (incident; 2π) and spherical (under-ice; 4π) quantum sensors (Lincoln, NE, USA), respectively, and a 4π:2π ratio was used to determine “pseudotransmissivity” (see Supporting Information: Appendix 1 for more details). Given that microalgal biomass is greatest near the ice-water interface, we focused our study on the bottom 10 cm of sea ice.

Biological samples were obtained from the bottom 10 cm of a single ice core by quickly removing the section with a cleaned handsaw. The section was sealed in a clean plastic bag and stored in a cooler in the dark until transport back to the lab. Samples from DOYs 120 and 139 differed from the 10 cm length and were 12 and 5-cm section lengths, respectively. Samples were processed by adding 100 ml of 0.2 µm filtered seawater cm^{-1} of ice to prevent osmotic shock (Garrison and Buck, 1986) and melted at 4 °C in the dark overnight. Once entirely melted, 1-2 aliquots (12-171 mL) of each sample were vacuum filtered ($\leq$ 5 psi) for chl *a* using 25 mm glass fiber filters (Whatman GF/F) after homogenization; filters were folded and inserted into glass vials, capped, and stored frozen until further processing (see Supporting Information: Appendix 1 for more details). The remaining sample volume was processed for DNA by filtering the sample onto a 0.2 µm Sterivex filter (Millipore Sigma) using a peristaltic pump and stored at -80 °C until further processing.

2.2. *DNA extraction, sequencing, and bioinformatic processing*

Sterivex filter cartridges were opened using ethanol cleaned PVC cutters, sliced and removed from their housing using ethanol cleaned scalpel and forceps. Filters were placed directly into 5-ml bead tubes containing lysis buffer and stored in the refrigerator until enough samples were available to proceed with extraction. DNA was extracted using the NucleoMag DNA/RNA Water kit (Macherey Nagel, Düren, GE) according to the manual for filters sized 47 mm. The V4 region of both the 16S and 18S rRNA genes were amplified for each sample. 16S rRNA gene amplicons were produced using the revised Earth Microbiome Project primers (515FB and 806RB; Caporaso et al. 2012; Apprill et al. 2015; Parada et al. 2016). 18S rRNA gene amplicons were generated using the primers TAReuk454FWD1 and TAReukREV3 (Stoeck et al., 2010). Primers were modified with TaggiMatrix indices to enable pooling of samples prior to adaptation

with Illumina sequencing adapters (Glenn et al., 2019). Samples were sequenced on an Illumina MiSeq with a 2 x 300 paired-end kit at the University of Alaska Fairbanks' Genomics Core Laboratory.

Sample libraries were initially demultiplexed and outer barcodes were removed as part of the standard Illumina post-processing. Sequenced samples were further demultiplexed, and internal indices removed, using the Mr. Demuxy package (Glenn et al., 2019). The QIIME2 (version 2023.5) workflow was used to process reads before further analysis (Caporaso et al., 2010). First, primer regions were removed using Cutadapt (Martin, 2011). Sequences were denoised and dereplicated using DADA2, including quality control, chimera checking and paired-end joining in R (Callahan et al., 2016). Base qualities were visually assessed, and sequences trimmed, when quality score of the 25th percentile reached 33. Denoising was conducted on "pseudo"-pooled samples for increased sensitivity. Chimeras were identified and removed from samples individually with a "—p-min-fold-parent-over-abundance" value of 2. Prokaryotic amplicon sequence variants (ASVs) were classified using a weighted classifier (515f-806r-average-classifier.qza) trained on the Silva 138.1 database (Quast et al., 2012; Bokulich et al., 2018; Kaehler et al., 2019; Robeson et al., 2021). A classifier was trained on the PR2 database (version 5.0.0) for eukaryotic ASV classification (Guillou et al., 2012). ASVs were identified to the lowest taxonomic level possible and ASVs of the same taxonomic identity were numbered sequentially (Table S1). The R package 'microViz' was used to standardize taxonomic naming when corrections were required with the "tax_fix()" command (Barnett et al., 2021). Non-target amplicons such as 16S sequences belonging to eukaryota, chloroplasts, mitochondria, or unassigned, and 18S sequences belonging to bacteria, metazoa, unassigned, or plastid DNA, were removed. Phyloseq was used for data manipulation and rarefaction prior to analyses; either rarified or unrarefied data were used dependent on the analysis. Prokaryotic and eukaryotic sequence data were rarefied to 10,497 and 15,684 reads per sample, respectively. Unrarefied data were converted to within sample relative abundance. Taxonomic corrections were made to the eukaryotic classifications due to classifier uncertainty and incomplete taxonomic representation in the PR2 database (Table S1). Each ASV involved with a significant parasitoid correlation was checked via NCBI BLAST alignment. All *Tryblionella* ASVs were reassigned to the genus *Nitzschia* and *Amphiprora* ASVs to the genus *Entomoneis*. All other changes were simple decreases in taxonomic resolution, e.g., *Attheya septentrionalis* to *Attheya* sp.

2.3 Bioinformatic analysis

Community structuring across our time-series was investigated according to Walker et al. (2023) for rarefied prokaryotic and eukaryotic ASV data. Briefly, the "ward.D2" method for hierarchical clustering was used to identify unique clusters (Murtagh and Legendre, 2014). The 'vegan' package was used to investigate cluster validity, within-cluster dispersion, and significant differences in composition between clusters using a silhouette test, dispersion test "betadisper," and PERMANOVA "adonis2", respectively (Oksanen et al., 2008). Community structure was visualized using non-metric multidimensional scaling (nMDS) using Bray-Curtis dissimilarity matrices with Wisconsin double standardization transformed ASV tables. Outliers were identified using Mahalanobis distance using 'rstatix' (Kassambara, 2023); outliers were retained on the nMDS plot but were excluded from cluster polygons.

Cluster association indices were calculated for each taxon to identify which taxa were significantly associated with each of the clusters. The 'indicspecies' package was used to

calculate the point biserial correlation coefficient on rarefied data (Cáceres and Legendre, 2009), and corrected for unequal sample distribution between clusters (Tichy and Chytry, 2006). Only taxa with $p < 0.001$, correlation coefficients >0.5, and contributed at least 0.5% of all sequences (16S or 18S) were retained.

Correlations between putative parasitoids and phototrophic hosts were investigated using Spearman's rank correlation of select ASVs using the 'psych' (Revelle, 2023; v.2.3.9) package in R with false discovery rate corrections for *p* values (Benjamini et al., 2009). Unrarefied relative abundance data were first centered log-ratio transformed using the 'SpiecEasi' package (v.1.1.3; Kurtz et al., 2017), after removal of rare taxa (occurring as <0.1% in fewer than 50% of samples). Parasitoids were limited to the classes Chytridiomycetes, Thecofilosea (Cercozoa), Labyrinthulomycetes (Bigyra), Oomycetes and Syndiniales (Dinoflagellata) while hosts were limited to the dominant phototrophs, i.e., diatoms (Bacillariophyceae, Mediophyceae, and Coscinodiscophyceae) and dinoflagellates (Dinophyceae). Correlation matrices were produced at the ASV level, retaining only those with at least a moderate correlation strength, i.e. |rho| <0.5; $p < 0.05$). We sampled again in April of 2022 and used microscopy to validate potential correlations (see Supporting Information: Appendix 1 for more details).

3. Results

Snow depth ranged from 0 to 6 cm during the study period, reaching a maximum on DOY 137 (Figs. 1c & S2b). Ice thickness was relatively uniform with a thickness of 109 ± 2 cm (mean ± SD) until melt onset, declining thereafter to a minimum thickness of 95 cm (Fig. S2c). Direct measurements of under-ice photosynthetically active radiation (PAR) ranged from 2.34 – 77.50 µmol photons m^{-2} d^{-1} (Fig. 1c) which was 0.25 – 11.13% of incident PAR (Fig. S2). The air temperature began warming on DOY 133 and reached above 0 °C on DOY 141 (Fig. S3a). The temperature measured at 2.5 cm from the bottom of the ice warmed above -1.8 °C by DOY 134, indicating the initiation of bottom ice melt between DOY 132 and 134 (Fig. S3d; ice growth < DOY 134). The brine salinity from the bottom 10 cm decreased substantially between DOYs 132 and 137 (Fig. S4c). The peak chlorophyll biomass occurred on DOY 128 (May 8th), reaching a maximum of 46.6 mg chl *a* m^{-2} (Fig. 1). The calculated accumulation and loss rates were 2.64 and -4.57 mg chl *a* m^2 d^{-1}, respectively. Areal chl *a* concentration declined below 1 mg m^{-2} on DOY 144 (May 24th); bloom phases are therefore defined as "bloom" <DOY 144 and "post-bloom" ≥DOY 144 (Fig. 1a). The average proportion of chlorophyll degradation product (phaeophytin) increased from 31% to 45% after the onset of bottom ice melt. Seawater nutrient concentrations peaked on the date of bloom termination (DOY 144; Fig. 1b). Bulk nutrient concentrations in the bottom 10 cm of ice were significantly correlated with chl *a*; nitrate (adj. r^2=0.45, p =0.0014), nitrite (adj. r^2=0.17, p =0.0447), ammonium (adj. r^2=0.36, p =0.0038), phosphate (adj. r^2=0.63, p <0.0001) and silicate (adj. r^2=0.41, p <0.0019; Fig. S5).

3.1.1. *Sympagic community composition patterns*

The total number of prokaryotic ASVs identified from the unrarefied data was 469, representing 124 families from 33 classes of bacteria and archaea. A relative abundance of approximately 48% of the sequence reads belonged to just two ASVs identified to the Genus level, *Oleispira* sp. and *Paraglaciecola* sp., 30% and 17.5%, respectively. *Polaribacter* was most abundant early in the time-series before transitioning to a bloom of *Oleispira* that approximately follows the microalgal bloom (Fig. 2). *Tenacibaculum* and *Colwellia* genera were the most abundant taxa in the post-bloom period (Fig. 2). The combined relative abundance of all four *Oleispira* ASVs

reached a peak of 84.4% on DOY 120 and was above 5% during a 35-d period (n=15); eight of those samples were above 50% (Fig. S6a). A positive correlation was found between *Oleispira* relative abundance and the areal chl *a* concentration (adj. r^2 = 0.68, p = <0.001; Fig. S6b). Three prokaryotic community clusters were identified as unique using hierarchical clustering analysis (adonis2: F = 8.59, $p < 0.001$), and was supported by a marginally insignificant within-cluster dispersion (betadisper: $p = 0.075$). The average silhouette width of 0.47 supports the separation of these clusters, referred to as clusters P1, P2, and P3 (Figs. 2a & S7a). Prokaryotic taxa associated with the clusters act as representatives for describing the major successional patterns and associated metabolisms (Table S3). *Polaribacter* was the dominant genus during the early-bloom (P1), preceding a bloom of *Oleispira* coincident with the microalgal bloom (P2), before transitioning to a more even post-bloom (P3) community represented by members of *Colwellia, Marinomonas,* and *Tenacibaculum*.

The total number of unicellular eukaryotic ASVs identified from the unrarefied data was 751, representing 14 divisions. The relative abundance of the top five most abundant classes contributed 75.4% of all sequences reads: Bacillariophyceae (26.5%), Dinophyceae (23.4%), Thecofilosea (13.8%), Oomycetes (6.8%), and the Imbricatea (4.9%). A total of 119 diatom ASVs contributed to 28% of the relative read abundance. The diatom genus *Nitzschia* contributed most to the bloom-phase, before transitioning into a post-bloom phase with a large contribution by the dinoflagellate genus *Heterocapsa* (Fig. 2d). Hierarchical clustering analysis identified two unique eukaryotic clusters (adonis2: F = 8.72, $p < 0.001$). The dendrogram indicated a substructure within these two major clusters (Fig. S7b). Within-cluster dispersion was not significant (betadisper: $p = 0.292$), and the average silhouette width of 0.27 is generally considered weak. We refer to these two clusters as E1 and E2, which are representative of sea-ice algal bloom and post-bloom periods, respectively (Fig. 1c). One outlier (DOY = 113) was identified using Mahalanobis distance but was included in all analyses, although excluded from the nMDS polygon (Fig. 2b). Eukaryotic association indices revealed taxa significantly associated with each of the two clusters (Table S4). Four diatom ASVs were associated with the bloom phase cluster (E1), while none were associated with post-bloom (E2).

3.1.2. *Parasitoid-host associations*

The putative parasitoids investigated in this study appear to follow successional co-exclusion during the sympagic algal bloom, seen by their relative abundance (Fig. 3). The Chytridiomycetes followed a rhythmic pattern of peaks and troughs, roughly following a single cycle approximately every seven days during the bloom period. The Thecofilosea had genera dependent development during the time series, *Cryothecomonas* peaked during the late-bloom period while *Protaspa* became most prevalent after *Cryothecomonas* declined. The unclassified Cryomonadida (Cercozoa, Thecofilosea), Labyrinthulomycetes and Syndiniales remained relatively low throughout the timeseries, while the relative abundance of Oomycetes dramatically increased during the post-bloom period. Directed correlations, i.e., parasitoid versus microalgal pairings, were investigated at the ASV level (Fig. 4). Of the 91 significant correlations, 75 were with ASVs of the Thecofilosea (62 of which were with diatoms). Using the combined positive and negative correlations as an indicator of host range, the thecofilosean parasitoids had the largest potential host range while the labyrinthulids were the most limited (Fig. 4). Special attention was given to the correlated ASV pairing of Lobulomycetales order 1 with *Nitzschia* genera (Fig. 5). Subsequent microscope observations support at least some of

the correlations that were found, and we provide for the first time evidence for internal parasitization in Arctic diatoms by *Cryothecomonas* (Fig. 6).

4. Discussion

4.1. *Physicochemical environment and bloom dynamics*

The maximum ice thickness of undeformed sea ice at Utqiaġvik has decreased by ~0.5 m compared to measurements from the early 2000's (Jin et al., 2006; Mahoney et al., 2007; Lee et al., 2008; Manes and Gradinger, 2009; Fig. S2). Snow depth in 2021 was also thinner than earlier measurements, which often reached ~20 cm (or greater in drifts; Herzfeld et al., 2006; Jin et al., 2006; Manes and Gradinger, 2009). The combination of these thinner snow and ice layers provided greater light transmittance than in past decades (Figs. 1c & S2). Calculated pseudotransmitted irradiances under the ice were below photoinhibitory thresholds until the post-bloom period (~50 µmol photons m^{-2}; Arrigo et al., 2010; Juhl and Krembs, 2010; Croteau et al., 2022; Dilliplaine and Hennon, 2023; Fig. S2e). However, excluding the chlorophyll layer from attenuation calculations revealed that photoinhibitory irradiances may have been experienced during the bloom by algae at the top of the dense ice algal layer (Fig. S2h). An overall brighter under-ice light field is likely to become more common as ice thins and less snow falls, which may influence community composition or the vertical distribution of species as they balance light and nutrient requirements and preferences (Aumack et al., 2014).

The underlying seawater nutrient concentration and flux are generally considered important factors controlling the magnitude of ice algal blooms (Cota et al., 1991; Gradinger, 2009; Rózańska et al., 2009). During our study, seawater nutrient concentrations (Fig. 1b) and nutrient ratios (Fig. S8) were similar to previous studies in the region during the spring ice-algal bloom (Lee et al., 2008; Manes and Gradinger, 2009). Nutrients remained replete in the underlying seawater throughout our sampling period, however, resupply is largely controlled by physical processes, i.e*.,* turbulence at the ice-water interface, which was not measured during this campaign. We excluded the use of sea-ice brine nutrient concentrations in our analysis because it appeared that cell lysis during the melt procedure resulted in the release of intracellular nutrient pools, evident by the significant correlation of each macronutrient analyte with chl *a* (Fig. S5). The observed nutrient ratios in underlying seawater were well below the expected 16:1 (N:P) from Redfield and greater than 1:1 (Si:N; Fig. S8), indicating nitrate resupply became the limiter to maximum biomass accumulation (Redfield et al., 1963) prior to the onset of melt. Using the empirical nitrate-chlorophyll relationship from Rózańska et al. (2009) the average seawater nitrate concentration (5.6 µmol L^{-1}) predicts a maximum chl *a* concentration of 44.9 mg m^2, closely matching our maximum observed concentration of 46.6 mg m^{-2} (Fig. 1a).

This study is the first to document the near-complete growth, decay, and fully realized magnitude of the sea-ice algal bloom at Utqiaġvik, AK, USA. The peak of the algal bloom occurred on DOY 128 (May 8th) similar to the peak date (DOY 121; May 1st) derived from regionally compiled data presented in Leu et al. (2015). The 2021 bloom peak exceeded all previously reported values near our study site. The highest prior measurement was 36.2 mg chl *a* m□², measured in late May (Gradinger et al., 2009), while our peak was ~25% greater than this isolated observation, and nearly 300% greater than the model estimate from compiled data (Leu et al., 2015). It remains unclear whether this elevated biomass reflects environmental change (e.g., thinning ice and snow, faster under-ice currents) or is due to higher temporal resolution. Sampling just one week before or after the actual peak would have underestimated

biomass by 26-38%, respectively. Bloom termination and succession were tightly linked to the onset of sea ice melt, consistent with previous observations (Leu et al., 2015 and references therein). Bottom-ice melt coincided with atmospheric warming, and the post-melt increase to phaeophytin proportion (Fig. 1a) indicated the onset of unfavorable conditions such as freshening, nutrient depletion, grazing, or infection.

4.2. *Sympagic community dynamics*

We observed distinct patterns of succession in eukaryotic and prokaryotic communities associated with bloom stage (Fig. 2). The eukaryotic community gradually transitioned between the bloom (E1) and post-bloom (E2) phases. The E1 cluster was enriched in pennate diatoms and transitioned to flagellate dominance in E2 (Fig. 2; Table S4), a well-established progression in Arctic sea ice (von Quillfeldt et al., 2003; Rózańska et al., 2009; Alou-Font et al., 2013). We observed three distinct prokaryotic community clusters, largely following the temporal evolution of the bloom: early- (P1), mid- (P2), and post-bloom (P3; Figs. 2a). Prokaryotic community composition is known to change over the course of microalgal blooms as the concentration and composition of organic matter shifts with bloom stage (Zhang et al., 2018; Zhou et al., 2018).

The E1 cluster was associated with the diatom genera *Nitzschia* and *Navicula,* which are among the most abundant algae in Arctic sea ice (Table S4; Leu et al., 2015). An unidentified cryomonad (Cryomonadida order 1) was also associated with E1 and Cryomonadida are commonly reported in Arctic sea ice and are generally considered heterotrophic (Thaler and Lovejoy, 2012). Rhythmic fluctuations of *Nitzschia* relative abundance were seemingly unrelated to environmental drivers. These fluctuations may be explained by spatial heterogeneity, or parasitoid dynamics as discussed in section 4.3.1.

The prokaryotic community succession was likely driven by changes in dissolved organic matter availability and composition. The P1 associated *Polaribacter*, and P3 associated *Tenacibaculum* and *Colwellia* ASVs, are heterotrophic bacteria known for their utilization of microalgal-derived dissolved organic matter (DOM; Landa et al., 2016; Underwood et al., 2019). *Colwellia* and *Tenacibaculum* are capable of degrading high molecular weight DOM; additionally, *Tenacibaculum* can utilize complex extracellular polymeric substances derived from diatom biofilms (Bohórquez et al., 2017; Underwood et al., 2019). *Marinomonas* which was also associated with the P3 cluster, has the capacity to metabolize aromatics from terrestrial peat (Sipler et al., 2017). These results suggest *Polaribacter* uses labile carbohydrates, while P3 members degrade recalcitrant high-molecular-weight substrates remaining after labile material is consumed.

Unexpectedly, the prokaryotic community during the mid-bloom (P2) was dominated by the oil-degrading bacterium *Oleispira* (Fig. S6; Table S3). Many sympagic prokaryotic genera have the capacity to degrade petroleum hydrocarbons, such as *Colwellia, Polaribacter, Nonlabens,* and *Paraglaciecola,* (Brakstad et al., 2008; Yang et al., 2016; Netzer et al., 2018). *Oleispira*, however, is considered an obligate hydrocarbonoclastic bacterium associated with the degradation of alkanes in cold water (Yakimov et al., 2003; Lofthus et al., 2018). *Oleispira* quickly blooms in response to petroleum contamination (Boccadoro et al., 2018) and relative contributions of *Oleispira* exceeding 5% are usually associated with hydrocarbon exposure (Krolicka et al., 2019). In our study, *Oleispira* exceeded 80% prokaryotic relative abundance in some samples, despite no obvious indications of hydrocarbon exposure (e.g., discoloration, sheen, odor) *Oleispira* enrichment in the water column, due to a distant spill, could have

advected under our ice station. Seawater flux into the bottom ice, along with physical sieving, could allow for the entrainment of seawater bacteria into the bottom ice layer (Syvertsen, 1991; Spindler, 1994). However, the close association of hydrocarbonoclastic bacteria, such as *Oleispira*, with phytoplankton (Thompson et al., 2020; this study), or decaying microalgae (Cono et al., 2022), warrants reevaluation of *Oleispira* as an indicator taxon of fossil hydrocarbon exposure, as these could be sources of biogenic hydrocarbons.

The eukaryotic E2 community was associated with heterotrophic flagellates and ciliates (Table S4) which has been previously documented in summer sea ice (Leu et al., 2015; Marquardt et al., 2023). Dinoflagellates in E2 included *Gymnodinium* and *Heterocapsa*. *Heterocapsa,* are common in water and sea ice throughout the Arctic (Rózańska et al., 2009; Rintala et al., 2010) and *Gymnodinium* spp. feed on small diatoms (Eddie et al., 2010) and are correlated with higher light conditions (Duncan et al., 2024). In addition to dinoflagellate taxa, ASVs of the Pyramimonodaophyte, *Pyramimonas sp.,* thecofilosean *Protaspa*, Oomycetes and Cilliophora were also associated with the E2 cluster. The green alga, *Pyramimonas*, sometimes forms dense blooms in under-ice brackish water ponds associated with melt conditions (Gradinger, 1996; Massicotte et al., 2020) and the heterotrophic flagellate *Protaspa* can feed on diatoms using pseudopodia (Schnepf and Kühn, 2000; Howe et al., 2011). The Oomycetes can be parasitic (Thines et al., 2015) or saprotrophic, thus their increased presence in the post-bloom community may represent an opportunity to feed on light and salinity stressed diatoms or on the post-bloom exopolymers that are preferentially retained during melt (Meiners et al., 2008; Juhl et al., 2011). The abundance of putative parasitoids both in bloom and post-bloom conditions was striking, leading us to further explore their potential role in shaping microalgal succession.

4.3. *Sea-ice parasitoid dynamics and potential host range*

To explore the relationship of parasitoid groups in shaping sea-ice communities, we identified putative parasitoid sequences from the following taxonomic groups: Chytridiomycetes (Fungi), Cryomonadida (Cercozoa, Thecofilosea)*,* Oomycetes*,* Syndiniales (Dinophyceae) and Labyrinthulomycetes (Bigyra). Within the Cryomonadida, the relationship between *Protaspa* and *Cryothecomonas* are not fully resolved, so both of these groups were retained in this study despite parasitism confined only to the *Cryothecomonas*. Our time-series data revealed successional patterns through the microalgal bloom (Fig. 3). Environmental controls on parasitoid infections remain poorly understood, aside from a few specific cases. Infections by the cryomonad *Cryothecomonas aestivalis* appear inhibited below 4 °C (Peacock et al., 2014; Catlett et al., 2023). Our observations demonstrate that parasitoid groups periodically spike, suggesting that infections are likely occurring throughout the spring bloom at temperatures below -1 °C (Fig. 3). Brine salinity varies more widely in the spring (Fig. S4c) and likely plays a key role in regulating parasitoid pathogenicity in sea ice. Chytridiomycetes were abundant during the early bloom but declined with melt onset and may be stenohaline, while cryomonads and Oomycetes may be euryhaline and tolerant of fresher meltwater (Fig. 3). However, previous studies report both cryomonads and chytrids as more common in phytoplankton influenced by sea-ice melt waters (Thaler and Lovejoy, 2012; Kilias et al., 2020), implying that the physical melting and flushing of the ice more strongly govern their presence. Stress due to excessive irradiance increases microalgal susceptibility to chytrid infection in sea ice (Hassett and Gradinger, 2016), and along with salinity stress, these factors may help shape parasitoid succession, as host susceptibility varies with time.

We analyzed 18S ASV time series data for significant correlations between putative parasitoids and potential hosts, assuming correlations could be positive or negative depending on the infection phase captured. Dinoflagellates showed far fewer correlations with putative parasitoids than diatoms, suggesting they are less likely hosts (Fig. 4). Among diatoms, *Navicula* and *Nitzschia* were both highly abundant and significantly correlated with parasitoids. This supports the “kill-the-winner” hypothesis which postulates that the most abundant taxa experience greater infection rates from viruses or parasitoids, particularly when these are diverse or have a broad host range (Thingstad, 2000; Abonyi et al., 2024). By suppressing dominant strains, parasitoids may promote microalgal coexistence and diversity, enhancing resilience to environmental change (Abonyi et al., 2024). This could be especially important in the space-limited brine channel system.

Chytridiomycetes were the most abundant parasitoid group during the algal bloom’s growth phase (Fig. 3a), consistent with previous observations (Donk and Ringelberg, 1983; Ibelings et al., 2004). These host-specific fungal parasites infect Arctic microalgae (Hassett and Gradinger, 2016) and exert top-down control, shaping bloom dynamics and succession. The chytrid ASV, Lobulomycetales order 1, was significantly correlated with a select few diatoms and dinoflagellates, including *Nitzschia* genus 4 (Fig. 4). However, their dynamics suggest temporal separation rather than infection (Fig. 5). *Nitzschia* genera 1 & 5, though not significant (p adj. > 0.05), showed strong correlations (rho ≥ 0.5) and dynamics resembling Lotka-Volterra patterns. *Nitzschia* genera (ASV 1 & 5) were negatively correlated with Lobulomycetales order 1 during the bloom phase, but were overall, positively correlated, due to post-bloom dynamics. It is therefore likely that we are missing true parasitoid-host interactions that were not significantly correlated while also identifying false positives. Similar inconsistencies in known parasitoid-host pairings have been difficult to parse from high-frequency long-term metabarcoding time-series data due to inconsistent dynamics. We suggest that *Nitzschia* spp. were primary chytrid hosts during our timeseries due to their contrasting peaks and troughs throughout the bloom. Although lifecycle data for marine chytrids are limited, the amphibian pathogen *Batrachochytrium dendrobatidis*, completes its lifecycle in ~4-5 days (Berger et al., 2005). In our time series, periodic chytrid peaks, and *Nitzschia* genera 1 & 5 dips (Figs. 3 & 5), offset by ~2 days for genus 5, suggest synchronized infection and zoospore release every ~7 days. We propose that chytrid peaks reflect sporangia attached to algal hosts retained during sampling, while dips reflect zoospore release and potential loss through brine drainage or dispersal into underlying water. These waves of infection support a cyclic interaction with *Nitzschia* spp. (Fig. 5), though microscopy, isolation, and co-culture are needed to confirm this lifecycle and host range.

Few correlations were found within the Labyrinthulomycetes (Fig. 4); though some thraustochytrids can parasitize diatoms (Hassett, 2020) their typical role is organic matter decomposition (Hassett and Gradinger, 2018). Oomycetes increased post-bloom, along with low levels of Syndiniales (Fig. 3d,e), both of which have a broad host range across Kingdoms (Käse et al., 2021). The order Syndiniales may be more important in underlying waters (Terrado et al., 2009; Marquardt et al., 2016; Kellogg et al., 2019; Jacquemot et al., 2022). Most oomycete ASVs (>85%) were unclassifiable beyond class level, as previously reported in Hassett et al. (2019). Their post-bloom increase may reflect saprotrophic breakdown of ice-retained carbon. However, a negative correlation with a *Cymbellales* ASV, supported by known *Lagena-Cymbella* interaction (Thines and Buaya, 2022), and sequence homology to *Diatomophthora drebesii*, a diatom parasitoid, suggest parasitic roles are probable. Given their relative abundance, Oomycetes may play a key role in Arctic biogeochemical as both degraders and parasitoids.

Cryomonadida (Thecofilosea) featured prominently in our parasitoid correlation matrix (Fig. 4), with some ASVs showing broad host associations among diatoms. *Cryothecomonas* and *Protaspa*, display two trophic modes: heterotrophy of small protists (Thaler and Lovejoy, 2012), and by internal parasitization of large diatoms (Drebes et al., 1996; Kühn et al., 2000). Correlated diatom hosts (e.g.: *Nitzschi*a and *Navicula* spp.) are typically large morphotypes within sea ice, consistent with *Cryothecomonas* hosts. Although *C. aestivalis* is a known diatom parasitoid (Drebes et al., 1996), Arctic *Cryothecomonas* spp*.* have only been observed as free-living grazers (Thaler and Lovejoy, 2012). In 2022, we observed an undescribed *Cryothecomonas* sp*.* actively parasitizing *Nitzschia* spp*.* (e.g.: *N. arctica* and *N. promare*), consuming the plastids and protoplasm and asexually reproducing (Fig. 6). Our correlation data suggests that several genera beyond *Nitzschia* and *Navicula* may also be hosts for cryomonads, though *C. aestivalis* is known to be host specific (Drebes et al., 1996; Schnepf and Kühn, 2000). *Protaspa*-host correlations were similar to *Cryothecomonas* suggesting potential host overlap or similar environmental response*.* As Cryomonadida are abundant in polar waters (Thomsen et al., 1991), their trophic role in sea ice warrants reevaluation in light of observed parasitization, particularly their influence on diatom dynamics and succession.

We found compelling evidence that the wide diversity of parasitoids observed in this study alter microalgal community composition, particularly of the most abundant sea-ice diatoms. Previous studies have found that, depending on the host species and the parasitoid size classes, carbon flux may be shunted to, or from, grazers (Rasconi et al., 2014). For example, cryomonads and chytrids may redirect carbon from large diatoms—typically too big for grazers like *Calanus glacialis*—into smaller, grazer-accessible forms such as flagellated cells, zoospores, or sporangia (Rasconi et al., 2014; Frenken et al., 2016; Cleary et al., 2017). Parasitoid infections in sea-ice may be prolific (pers. obs) due to the dense microalgal concentrations in the confined brine channels. Parasitoid epidemics may suppress microalgal blooms leading to patchiness, and shift microalgal composition and while increasing diversity (Donk and Ringelberg, 1983; Frenken et al., 2016).

5. Conclusions

As Arctic warming continues, monitoring the timing and magnitude of vernal ice-algal blooms is crucial for understanding the ecosystem response to environmental change. High-frequency sampling of landfast sea ice near Utqiaġvik, Alaska in 2021 captured the full bloom cycle, revealing a much larger magnitude relative to prior observations, and highlighting the importance of nitrate limitation in constraining biomass accumulation, and physical forcing (melt onset) on terminating the bloom. Parasitoids emerged as major contributors to the eukaryotic microbial community. We report many potential associations of diatoms with *Cryothecomonas,* including the first observation of parasitic behavior in sea ice, and suggest chytrid-linked declines in *Nitzschia*. Understanding the complex dynamics of parasitoids within the sea-ice ecosystem is crucial to elucidate their role in shaping microbial communities, nutrient cycles, and broader ecological interactions. These findings support the potential role of parasitoids in regulating dominant microalgae through "kill-the-winner" dynamics (Thingstad, 2000; Abonyi et al., 2024), promoting coexistence and microbial diversity by freeing space within the constrained brine channel system for other taxa. As a result, parasitoids may enhance resilience through increased diversity at the base of the sea-ice food web – a critical component of the rapidly changing Arctic ecosystem.

References

Abonyi, A, Fornberg, J, Rasconi, S, Ptacnik, R, Kainz, MJ, Lafferty, KD. 2024. The chytrid insurance hypothesis: integrating parasitic chytrids into a biodiversity–ecosystem functioning framework for phytoplankton–zooplankton population dynamics. *Oecologia* **204**(2): 279–288. doi: 10.1007/s00442-024-05519-w

Alou-Font, E, Mundy, C, Roy, S, Gosselin, M, Agustí, S. 2013. Snow cover affects ice algal pigment composition in the coastal Arctic ocean during spring. *Marine Ecology Progress Series* **474**: 89–104. doi: 10.3354/meps10107

Ambrose, WG, Quillfeldt, C von, Clough, LM, Tilney, PVR, Tucker, T. 2005. The sub-ice algal community in the Chukchi Sea: large- and small-scale patterns of abundance based on images from a remotely operated vehicle. *Polar Biology* **28**(10): 784–795. doi: 10.1007/s00300-005-0002-8

Amundsen, P, Lafferty, KD, Knudsen, R, Primicerio, R, Klemetsen, A, Kuris, AM. 2009. Food web topology and parasites in the pelagic zone of a subArctic lake. *Journal of Animal Ecology* **78**(3): 563–572. doi: 10.1111/j.1365-2656.2008.01518.x

Apprill, A, McNally, S, Parsons, R, Weber, L. 2015. Minor revision to V4 region SSU rRNA 806R gene primer greatly increases detection of SAR11 bacterioplankton. *Aquatic Microbial Ecology* **75**(2): 129–137. doi: 10.3354/ame01753

Arrigo, KR, Mills, MM, Kropuenske, LR, van Dijken, GL, Alderkamp, A-C, Robinson, DH. 2010. Photophysiology in two major Southern Ocean phytoplankton taxa: photosynthesis and growth of *Phaeocystis antarctica* and *Fragilariopsis cylindrus* under different irradiance levels. *Integrative and Comparative Biology* **50**(6): 950–966. doi: 10.1093/icb/icq021

Aumack, CF, Juhl, AR, Krembs, C. 2014. Diatom vertical migration within land-fast Arctic sea ice. *Journal of Marine Systems* **139**: 496–504. doi: 10.1016/j.jmarsys.2014.08.013

Babb, DG, Galley, RJ, Howell, SEL, Landy, JC, Stroeve, JC, Barber, DG. 2022. Increasing multiyear sea ice loss in the Beaufort Sea: a new export pathway for the diminishing multiyear ice cover of the Arctic Ocean. *Geophysical Research Letters* **49**(9): 1–11. doi: 10.1029/2021GL097595

Barnett, D, Arts, I, Penders, J. 2021. MicroViz: an R package for microbiome data visualization and statistics. *Journal of Open Source Software* **6**(63): 3201. doi: 10.21105/joss.03201

Benjamini, Y, Heller, R, Yekutieli, D. 2009. Selective inference in complex research. *Philosophical Transactions of the Royal Society A: Mathematical, Physical and Engineering Sciences* **367**(1906): 4255–4271. doi: 10.1098/rsta.2009.0127

Berger, L, Hyatt, A, Speare, R, Longcore, J. 2005. Life cycle stages of the amphibian chytrid *Batrachochytrium dendrobatidis*. *Diseases of Aquatic Organisms* **68**(1): 51–63. doi: 10.3354/dao068051

Bintanja, R, Selten, FM. 2014. Future increases in Arctic precipitation linked to local evaporation and sea-ice retreat. *Nature* **509**(7501): 479–482. doi: 10.1038/nature13259

Boccadoro, C, Krolicka, A, Receveur, J, Aeppli, C, Le Floch, S. 2018. Microbial community response and migration of petroleum compounds during a sea-ice oil spill experiment in Svalbard. *Marine Environmental Research* **142**(September): 214–233. doi: 10.1016/j.marenvres.2018.09.007

Boetius, A, Albrecht, S, Bakker, K, Bienhold, C, Felden, J, Fernández-Méndez, M, Hendricks, S, Katlein, C, Lalande, C, Krumpen, T, Nicolaus, M, Peeken, I, Rabe, B, Rogacheva, A, Rybakova, E, Somavilla, R, Wenzhöfer, F. 2013. Export of algal biomass from the melting Arctic sea ice. *Science* **339**(6126): 1430–1432. doi: 10.1126/science.1231346

Bohórquez, J, McGenity, TJ, Papaspyrou, S, García-Robledo, E, Corzo, A, Underwood, GJC. 2017. Different types of diatom-derived extracellular polymeric substances drive changes in heterotrophic bacterial communities from intertidal sediments. *Frontiers in Microbiology* **8**(FEB). doi: 10.3389/fmicb.2017.00245

Bokulich, NA, Kaehler, BD, Rideout, JR, Dillon, M, Bolyen, E, Knight, R, Huttley, GA, Gregory Caporaso, J. 2018. Optimizing taxonomic classification of marker-gene amplicon sequences with QIIME 2's q2-feature-classifier plugin. *Microbiome* **6**(1): 90. doi: 10.1186/s40168-018-0470-z

Brakstad, OG, Nonstad, I, Faksness, L-G, Brandvik, PJ. 2008. Responses of microbial communities in Arctic sea ice after contamination by crude petroleum oil. *Microbial Ecology* **55**(3): 540–552. doi: 10.1007/s00248-007-9299-x

Cáceres, M De, Legendre, P. 2009. Associations between species and groups of sites: indices and statistical inference. *Ecology* **90**(12): 3566–3574. doi: 10.1890/08-1823.1

Callahan, BJ, Mcmurdie, PJ, Rosen, MJ, Han, AW, A, AJ. 2016. DADA2: high resolution sample inference from Illumina amplicon data. *Nat Methods* **13**(7): 581–583. doi: 10.1038/nmeth.3869.DADA2

Caporaso, JG, Kuczynski, J, Stombaugh, J, Bittinger, K, Bushman, FD, Costello, EK, Fierer, N, Peña, AG, Goodrich, JK, Gordon, JI, et al. 2010. QIIME allows analysis of high-throughput community sequencing data. *Nature Methods* **7**(5): 335–336. doi: 10.1038/nmeth.f.303

Caporaso, JG, Lauber, CL, Walters, WA, Berg-Lyons, D, Huntley, J, Fierer, N, Owens, SM, Betley, J, Fraser, L, Bauer, M, Gormley, N, Gilbert, JA, Smith, G, Knight, R. 2012. Ultra-high-throughput microbial community analysis on the Illumina HiSeq and MiSeq platforms. *The ISME Journal* **6**(8): 1621–1624. doi: 10.1038/ismej.2012.8

Catlett, D, Peacock, EE, Crockford, ET, Futrelle, J, Batchelder, S, Stevens, BLF, Gast, RJ, Zhang, WG, Sosik, HM. 2023. Temperature dependence of parasitoid infection and abundance of a diatom revealed by automated imaging and classification. *Proceedings of the National Academy of Sciences* **120**(28): 2017. doi: 10.1073/pnas.2303356120

Chambouvet, A, Morin, P, Marie, D, Guillou, L. 2008. Control of toxic marine dinoflagellate blooms by serial parasitic killers. *Science* **322**(5905): 1254–1257. doi: 10.1126/science.1164387

Cleary, AC, Søreide, JE, Freese, D, Niehoff, B, Gabrielsen, TM. 2017. Feeding by *Calanus glacialis* in a high Arctic fjord: potential seasonal importance of alternative prey. Fields D, editor. *ICES Journal of Marine Science* **74**(7): 1937–1946. doi: 10.1093/icesjms/fsx106

Cono, V La, Smedile, F, Crisafi, F, Marturano, L, Toshchakov, S V., Spada, G La, Bản, NK, Yakimov, MM. 2022. Wintertime simulations induce changes in the structure, diversity and function of Antarctic sea ice-associated microbial communities. *Microorganisms* **10**(3): 623. doi: 10.3390/microorganisms10030623

Cota, G., Legendre, L, Gosselin, M, Ingram, R. 1991. Ecology of bottom ice algae: I. Environmental controls and variability. *Journal of Marine Systems* **2**(3–4): 257–277. doi:

10.1016/0924-7963(91)90036-T

Cota, GF, Anning, JL, Watson, NHF, Prinsenberg, SJ, Bennett, EB, Lewis, MR. 1987. Nutrient fluxes during extended blooms of Arctic ice algae. *Journal of Geophysical Research* **92**: 1951. doi: 10.1029/JC092iC02p01951

Cota, GF, Smith, REH. 1991. Ecology of bottom ice algae: II. Dynamics, distributions and productivity. *Journal of Marine Systems* **2**(3–4): 279–295. doi: 10.1016/0924-7963(91)90037-U

Croteau, D, Lacour, T, Schiffrine, N, Morin, PI, Forget, MH, Bruyant, F, Ferland, J, Lafond, A, Campbell, DA, Tremblay, JÉ, Babin, M, Lavaud, J. 2022. Shifts in growth light optima among diatom species support their succession during the spring bloom in the arctic. *Journal of Ecology* **110**(6): 1356–1375. doi: 10.1111/1365-2745.13874

Dilliplaine, K, Hennon, G. 2023. Impacts of crude oil on Arctic sea-ice diatoms modified by irradiance. *Elem Sci Anth* **11**(1): 1–21. doi: 10.1525/elementa.2023.00074

Donk, E van, Ringelberg, J. 1983. The effect of fungal parasitism on the succession of diatoms in lake Maarsseveen I (The Netherlands). *Freshwater Biology* **13**(3): 241–251. doi: 10.1111/j.1365-2427.1983.tb00674.x

Drebes, G, Kühn, SF, Gmelch, A, Schnepf, E. 1996. *Cryothecomonas aestivalis* sp. nov., a colourless nanoflagellate feeding on the marine centric diatom *Guinardia delicatula* (Cleve) Hasle. *Helgoländer Meeresuntersuchungen* **50**(4): 497–515. doi: 10.1007/BF02367163

Duncan, RJ, Søreide, JE, Varpe, Ø, Wiktor, J, Pitusi, V, Runge, E, Petrou, K. 2024. Spatio-temporal dynamics in microalgal communities in Arctic land-fast sea ice. *Progress in Oceanography* **224**(April 2023): 103248. doi: 10.1016/j.pocean.2024.103248

Dupont, F. 2012. Impact of sea-ice biology on overall primary production in a biophysical model of the pan-Arctic Ocean. *Journal of Geophysical Research: Oceans* **117**(C8): n/a-n/a. doi: 10.1029/2011JC006983

Eddie, B, Juhl, A, Krembs, C, Baysinger, C, Neuer, S. 2010. Effect of environmental variables on eukaryotic microbial community structure of land-fast Arctic sea ice. *Environmental Microbiology* **12**(3): 797–809. doi: 10.1111/j.1462-2920.2009.02126.x

Frenken, T, Velthuis, M, de Senerpont Domis, LN, Stephan, S, Aben, R, Kosten, S, van Donk, E, Van de Waal, DB. 2016. Warming accelerates termination of a phytoplankton spring bloom by fungal parasites. *Global Change Biology* **22**(1): 299–309. doi: 10.1111/gcb.13095

Garrison, DL, Buck, KR. 1986. Organism losses during ice melting: a serious bias in sea ice community studies. *Polar Biology* **6**(4): 237–239. doi: 10.1007/BF00443401

Garrison, DL, Buck, KR, Fryxell, GA. 1987. Algal assemblages in Antarctic pack ice and in ice-edge plankton. *Journal of Phycology* **23**(4): 564–572. doi: 10.1111/j.1529-8817.1987.tb04206.x

Glenn, TC, Pierson, TW, Bayona-Vásquez, NJ, Kieran, TJ, Hoffberg, SL, Thomas, JC, Lefever, DE, Finger, JW, Gao, B, Bian, X, et al. 2019. Adapterama II: universal amplicon sequencing on Illumina platforms (TaggiMatrix). *PeerJ* **2019**(10). doi: 10.7717/peerj.7786

Gosselin, M, Legendre, L. 1990. Light and nutrient limitation of sea-ice microalgae (Hudson Bay, Canadian Arctic). Journal of Phycology. doi: 10.1016/S0198-0254(06)80482-6

Gosselin, M, Levasseur, M, Wheeler, PA, Horner, RA, Booth, BC. 1997. New measurements of phytoplankton and ice algal production in the Arctic Ocean. *Deep-Sea Research Part II: Topical Studies in Oceanography* **44**(8): 1623–1644. doi: 10.1016/S0967-0645(97)00054-4

Gradinger, R. 1996. Occurrence of an algal bloom under Arctic pack ice. *Marine Ecology Progress Series* **131**(1–3): 301–305. doi: 10.3354/meps131301

Gradinger, R. 2009. Sea-ice algae: major contributors to primary production and algal biomass in the Chukchi and Beaufort seas during May/June 2002. *Deep Sea Research Part II: Topical Studies in Oceanography* **56**(17): 1201–1212. doi: 10.1016/j.dsr2.2008.10.016

Gradinger, R, Kaufman, M, Bluhm, B. 2009. Pivotal role of sea ice sediments in the seasonal development of near-shore Arctic fast ice biota. *Marine Ecology Progress Series* **394**: 49–63. doi: 10.3354/meps08320

Guillou, L, Bachar, D, Audic, S, Bass, D, Berney, C, Bittner, L, Boutte, C, Burgaud, G, de Vargas, C, Decelle, J, et al. 2012. The Protist Ribosomal Reference Database (PR2): a catalog of unicellular eukaryote small sub-unit rRNA sequences with curated taxonomy. *Nucleic Acids Research* **41**(D1): D597–D604. doi: 10.1093/nar/gks1160

Hassett, BT. 2020. A widely distributed thraustochytrid parasite of diatoms isolated from the Arctic represents a gen. and sp. nov. *Journal of Eukaryotic Microbiology* **67**(4): 480–490. doi: 10.1111/jeu.12796

Hassett, B. T., Borrego, EJ, Vonnahme, TR, Rämä, T, Kolomiets, M V., Gradinger, R. 2019. Arctic marine fungi: biomass, functional genes, and putative ecological roles. *ISME Journal* **13**(6): 1484–1496. doi: 10.1038/s41396-019-0368-1

Hassett, BT, Gradinger, R. 2016. Chytrids dominate Arctic marine fungal communities. *Environmental Microbiology* **18**(6): 2001–2009. doi: 10.1111/1462-2920.13216

Hassett, BT, Gradinger, R. 2018. New species of saprobic Labyrinthulea (=Labyrinthulomycota) and the erection of a gen. nov. to resolve molecular polyphyly within the aplanochytrids. *Journal of Eukaryotic Microbiology* **65**(4): 475–483. doi: 10.1111/jeu.12494

Hassett, Brandon T, Thines, M, Buaya, A, Ploch, S, Gradinger, R. 2019. A glimpse into the biogeography, seasonality, and ecological functions of Arctic marine Oomycota. *IMA Fungus* **10**(1): 6. doi: 10.1186/s43008-019-0006-6

Herzfeld, UC, Maslanik, JA, Sturm, M. 2006. Geostatistical characterization of snow-depth structures on sea ice near Point Barrow, Alaska—a contribution to the AMSR-Ice03 field validation campaign. *IEEE Transactions on Geoscience and Remote Sensing* **44**(11): 3038–3056. doi: 10.1109/TGRS.2006.883349

Howe, AT, Bass, D, Scoble, JM, Lewis, R, Vickerman, K, Arndt, H, Cavalier-Smith, T. 2011. Novel cultured protists identify deep-branching environmental DNA clades of Cercozoa: new genera *Tremula*, *Micrometopion*, *Minimassisteria*, *Nudifila*, *Peregrinia*. *Protist* **162**(2): 332–372. doi: 10.1016/j.protis.2010.10.002

Ibelings, BW, De Bruin, A, Kagami, M, Rijkeboer, M, Brehm, M, Donk, E Van. 2004. Host parasite interactions between freshwater phytoplankton and chytrid fungi (Chytridiomycota). *Journal of Phycology* **40**(3): 437–453. doi: 10.1111/j.1529-8817.2004.03117.x

Jacquemot, L, Vigneron, A, Tremblay, J-É, Lovejoy, C. 2022. Contrasting sea ice conditions shape microbial food webs in Hudson Bay (Canadian Arctic). *ISME Communications* **2**(1):

1–10. doi: 10.1038/s43705-022-00192-7

Jin, M, Deal, CJ, Wang, J, Shin, K-H, Tanaka, N, Whitledge, TE, Lee, SH, Gradinger, RR. 2006. Controls of the landfast ice–ocean ecosystem offshore Barrow, Alaska. *Annals of Glaciology* **44**: 63–72. doi: 10.3189/172756406781811709

Juhl, A, Krembs, C, Meiners, K. 2011. Seasonal development and differential retention of ice algae and other organic fractions in first-year Arctic sea ice. *Marine Ecology Progress Series* **436**: 1–16. doi: 10.3354/meps09277

Juhl, AR, Krembs, C. 2010. Effects of snow removal and algal photoacclimation on growth and export of ice algae. *Polar Biology* **33**(8): 1057–1065. doi: 10.1007/s00300-010-0784-1

Juul-Pedersen, T, Michel, C, Gosselin, M, Seuthe, L. 2008. Seasonal changes in the sinking export of particulate material under first-year sea ice on the Mackenzie Shelf (Western Canadian Arctic). *Marine Ecology Progress Series* **353**: 13–25. doi: 10.3354/meps07165

Kaehler, BD, Bokulich, NA, McDonald, D, Knight, R, Caporaso, JG, Huttley, GA. 2019. Species abundance information improves sequence taxonomy classification accuracy. *Nature Communications* **10**(1): 4643. doi: 10.1038/s41467-019-12669-6

Käse, L, Metfies, K, Neuhaus, S, Boersma, M, Wiltshire, KH, Kraberg, AC. 2021. Host-parasitoid associations in marine planktonic time series: can metabarcoding help reveal them? Amato A, editor. *PLOS ONE* **16**(1): e0244817. doi: 10.1371/journal.pone.0244817

Kassambara, A. 2023. rstatix: pipe-friendly framework for basic statistical tests. Available at https://rpkgs.datanovia.com/rstatix/.

Kellogg, CTE, McClelland, JW, Dunton, KH, Crump, BC. 2019. Strong seasonality in Arctic estuarine microbial food webs. *Frontiers in Microbiology* **10**(November). doi: 10.3389/fmicb.2019.02628

Kilias, ES, Junges, L, Šupraha, L, Leonard, G, Metfies, K, Richards, TA. 2020. Chytrid fungi distribution and co-occurrence with diatoms correlate with sea ice melt in the arctic ocean. *Communications Biology* **3**(1): 183. doi: 10.1038/s42003-020-0891-7

Krolicka, A, Boccadoro, C, Nilsen, MM, Demir-Hilton, E, Birch, J, Preston, C, Scholin, C, Baussant, T. 2019. Identification of microbial key-indicators of oil contamination at sea through tracking of oil biotransformation: an Arctic field and laboratory study. *Science of the Total Environment* **696**: 133715. doi: 10.1016/j.scitotenv.2019.133715

Kühn, S, Lange, M, Medlin, LK. 2000. Phylogenetic position of *Cryothecomonas* inferred from nuclear-encoded small subunit ribosomal RNA. *Protist* **151**(4): 337–345. doi: 10.1078/S1434-4610(04)70032-2

Kurtz, Z, Mueller, C, Miraldi, E, Bonneau, R. 2017. SpiecEasi: sparse inverse covariance for ecological statistical inference.

Landa, M, Blain, S, Christaki, U, Monchy, S, Obernosterer, I. 2016. Shifts in bacterial community composition associated with increased carbon cycling in a mosaic of phytoplankton blooms. *The ISME Journal* **10**(1): 39–50. doi: 10.1038/ismej.2015.105

Lee, SH, Whitledge, TE, Kang, SH. 2008. Spring time production of bottom ice algae in the landfast sea ice zone at Barrow, Alaska. *Journal of Experimental Marine Biology and Ecology* **367**(2): 204–212. doi: 10.1016/j.jembe.2008.09.018

Leu, E, Mundy, CJ, Assmy, P, Campbell, K, Gabrielsen, TM, Gosselin, M, Juul-Pedersen, T, Gradinger, R. 2015. Arctic spring awakening - steering principles behind the phenology of vernal ice algal blooms. *Progress in Oceanography* **139**: 151–170. doi: 10.1016/j.pocean.2015.07.012

Litchman, E, Edwards, KF, Klausmeier, CA. 2015. Microbial resource utilization traits and trade-offs: implications for community structure, functioning, and biogeochemical impacts at present and in the future. *Frontiers in Microbiology* **6**(APR): 1–10. doi: 10.3389/fmicb.2015.00254

Litchman, E, de Tezanos Pinto, P, Edwards, KF, Klausmeier, CA, Kremer, CT, Thomas, MK. 2015. Global biogeochemical impacts of phytoplankton: a trait-based perspective. *Journal of Ecology* **103**(6): 1384–1396. doi: 10.1111/1365-2745.12438

Lizotte, MP. 2001. The contributions of sea ice algae to Antarctic marine primary production. **41**(1): 57–73.

Lofthus, S, Netzer, R, Lewin, AS, Heggeset, TMB, Haugen, T, Brakstad, OG. 2018. Biodegradation of n-alkanes on oil–seawater interfaces at different temperatures and microbial communities associated with the degradation. *Biodegradation* **29**(2): 141–157. doi: 10.1007/s10532-018-9819-z

Mahoney, A, Eicken, H, Shapiro, L. 2007. How fast is landfast sea ice? A study of the attachment and detachment of nearshore ice at Barrow, Alaska. *Cold Regions Science and Technology* **47**(3): 233–255. doi: 10.1016/j.coldregions.2006.09.005

Manes, SS, Gradinger, R. 2009. Small scale vertical gradients of Arctic ice algal photophysiological properties. *Photosynthesis Research*(102): 53–66. doi: 10.1007/s11120-009-9489-0

Marquardt, M, Goraguer, L, Assmy, P, Bluhm, BA, Aaboe, S, Down, E, Patrohay, E, Edvardsen, B, Tatarek, A, Smoła, Z, Wiktor, J, Gradinger, R. 2023. Seasonal dynamics of sea-ice protist and meiofauna in the northwestern Barents Sea. *Progress in Oceanography* **218**(September): 103128. doi: 10.1016/j.pocean.2023.103128

Marquardt, M, Vader, A, Stübner, EI, Reigstad, M, Gabrielsen, TM. 2016. Strong seasonality of marine microbial eukaryotes in a high-arctic fjord (Isfjorden, in west Spitsbergen, Norway). Stams AJM, editor. *Applied and Environmental Microbiology* **82**(6): 1868–1880. doi: 10.1128/AEM.03208-15

Martin, M. 2011. Cutadapt removes adapter sequences from high-throughput sequencing reads. *EMBnet.journal* **17**(1): 10. doi: 10.14806/ej.17.1.200

Massicotte, P, Amiraux, R, Amyot, M-P, Archambault, P, Ardyna, M, Arnaud, L, Artigue, L, Aubry, C, Ayotte, P, Bécu, G, et al. 2020. Green edge ice camp campaigns: understanding the processes controlling the under-ice Arctic phytoplankton spring bloom. *Earth System Science Data* **12**(1): 151–176. doi: 10.5194/essd-12-151-2020

Mcdonald, S, Koulis, T, Ehn, J, Campbell, K, Gosselin, M, Mundy, CJ. 2015. A functional regression model for predicting optical depth and estimating attenuation coefficients in sea-ice covers near Resolute Passage, Canada. *Annals of Glaciology* **56**(69): 147–154. doi: 10.3189/2015AoG69A004

Meiners, K, Krembs, C, Gradinger, R. 2008. Exopolymer particles: microbial hotspots of enhanced bacterial activity in Arctic fast ice (Chukchi sea). *Aquatic Microbial Ecology*

52(2): 195–207. doi: 10.3354/ame01214

Mortenson, E, Steiner, N, Monahan, AH, Hayashida, H, Sou, T, Shao, A. 2020. Modeled impacts of sea ice exchange processes on Arctic Ocean carbon uptake and acidification (1980–2015). *Journal of Geophysical Research: Oceans* **125**(7): 1–20. doi: 10.1029/2019JC015782

Murtagh, F, Legendre, P. 2014. Ward's hierarchical agglomerative clustering method: which algorithms implement ward's criterion? *Journal of Classification* **31**(3): 274–295. doi: 10.1007/s00357-014-9161-z

Netzer, R, Henry, IA, Ribicic, D, Wibberg, D, Brönner, U, Brakstad, OG. 2018. Petroleum hydrocarbon and microbial community structure successions in marine oil-related aggregates associated with diatoms relevant for Arctic conditions. *Marine Pollution Bulletin* **135**(March): 759–768. doi: 10.1016/j.marpolbul.2018.07.074

Oksanen, J, Kindt, R, Legendre, P, O'Hara, B, Simpson, GL, Solymos, PM, Stevens, MHH, & Wagner, H. 2008. The vegan package. *Community ecology package*(January): 190. Available at https://bcrc.bio.umass.edu/biometry/images/8/85/Vegan.pdf.

Parada, AE, Needham, DM, Fuhrman, JA. 2016. Every base matters: assessing small subunit rRNA primers for marine microbiomes with mock communities, time series and global field samples. *Environmental Microbiology* **18**(5): 1403–1414. doi: 10.1111/1462-2920.13023

Peacock, E, Olson, R, Sosik, H. 2014. Parasitic infection of the diatom *Guinardia delicatula*, a recurrent and ecologically important phenomenon on the New England Shelf. *Marine Ecology Progress Series* **503**: 1–10. doi: 10.3354/meps10784

Pineault, S, Tremblay, J, Gosselin, M, Thomas, H, Shadwick, E. 2013. The isotopic signature of particulate organic C and N in bottom ice: key influencing factors and applications for tracing the fate of ice algae in the Arctic ocean. *Journal of Geophysical Research: Oceans* **118**(1): 287–300. doi: 10.1029/2012JC008331

Quast, C, Pruesse, E, Yilmaz, P, Gerken, J, Schweer, T, Yarza, P, Peplies, J, Glöckner, FO. 2012. The SILVA ribosomal RNA gene database project: improved data processing and web-based tools. *Nucleic Acids Research* **41**(D1): D590–D596. doi: 10.1093/nar/gks1219

von Quillfeldt, CH, Ambrose, WG, Clough, LM. 2003. High number of diatom species in first-year ice from the Chukchi sea. *Polar Biology* **26**(12): 806–818. doi: 10.1007/s00300-003-0549-1

Rasconi, S, Grami, B, Niquil, N, Jobard, M, Sime-Ngando, T. 2014. Parasitic chytrids sustain zooplankton growth during inedible algal bloom. *Frontiers in Microbiology* **5**(MAY): 1–19. doi: 10.3389/fmicb.2014.00229

Redfield, A, Ketchum, B, Richards, F. 1963. The influence of organisms on the composition of sea-water. In: *The Sea*. p. 26–77.

Revelle, W. 2023. Psych: procedures for psychological, psychometric, and personality research. Available at https://cran.r-project.org/package=psych.

Rintala, J-M, Hällfors, H, Hällfors, S, Hällfors, G, Majaneva, M, Blomster, J. 2010. *Heterocapsa arctica* subsp. *frigida* subsp. nov. (Peridiniales, Dinophyceae)-description of a new dinoflagellate and its occurrent in the Baltic Sea. *Journal of Phycology* **46**(4): 751–762. doi: 10.1111/j.1529-8817.2010.00868.x

Robeson, MS, O'Rourke, DR, Kaehler, BD, Ziemski, M, Dillon, MR, Foster, JT, Bokulich, NA. 2021. RESCRIPt: reproducible sequence taxonomy reference database management. Pertea M, editor. *PLOS Computational Biology* **17**(11): e1009581. doi: 10.1371/journal.pcbi.1009581

Rózańska, M, Gosselin, M, Poulin, M, Wiktor, J, Michel, C. 2009. Influence of environmental factors on the development of bottom ice protist communities during the winter–spring transition. *Marine Ecology Progress Series* **386**: 43–59. doi: 10.3354/meps08092

Schnepf, E, Kühn, SF. 2000. Food uptake and fine structure of *Cryothecomonas longipes* sp. nov., a marine nanoflagellate incertae sedis feeding phagotrophically on large diatoms. *Helgoland Marine Research* **54**(1): 18–32. doi: 10.1007/s101520050032

Sipler, RE, Kellogg, CTE, Connelly, TL, Roberts, QN, Yager, PL, Bronk, DA. 2017. Microbial community response to terrestrially derived dissolved organic matter in the coastal Arctic. *Frontiers in Microbiology* **8**(JUN): 1–19. doi: 10.3389/fmicb.2017.01018

Skovgaard, A. 2014. Dirty tricks in the plankton: diversity and role of marine parasitic protists. *Acta Protozoologica* **53**(1): 51–62. doi: 10.4467/16890027AP.14.006.1443

Smith, REH, Harrison, WG, Harris, LR, Herman, AW. 1990. Vertical fine structure of particulate matter and nutrients in sea ice of the high Arctic. *Canadian Journal of Fisheries and Aquatic Sciences* **47**(7): 1348–1355. doi: 10.1139/f90-154

Spindler, M. 1994. Notes on the biology of sea ice in the Arctic and Antarctic. *Polar Biology* **14**(5): 319–324. doi: 10.1007/BF00238447

Stoeck, T, Bass, D, Nebel, M, Christen, R, Jones, MDM, Breiner, H-W, Richards, TA. 2010. Multiple marker parallel tag environmental DNA sequencing reveals a highly complex eukaryotic community in marine anoxic water. *Molecular Ecology* **19**(SUPPL. 1): 21–31. doi: 10.1111/j.1365-294X.2009.04480.x

Stroeve, J, Notz, D. 2018. Changing state of Arctic sea ice across all seasons. *Environmental Research Letters* **13**(10): 103001. doi: 10.1088/1748-9326/aade56

Syvertsen, EE. 1991. Ice algae in the Barents Sea: types of assemblages, origin, fate and role in the ice-edge phytoplankton bloom. *Polar Research* **10**(1): 277–288. doi: 10.1111/j.1751-8369.1991.tb00653.x

Terrado, R, Vincent, W, Lovejoy, C. 2009. Mesopelagic protists: diversity and succession in a coastal Arctic ecosystem. *Aquatic Microbial Ecology* **56**(1): 25–39. doi: 10.3354/ame01327

Thaler, M, Lovejoy, C. 2012. Distribution and diversity of a protist predator *Cryothecomonas* (Cercozoa) in Arctic marine waters. *Journal of Eukaryotic Microbiology* **59**(4): 291–299. doi: 10.1111/j.1550-7408.2012.00631.x

Thines, M, Buaya, AT. 2022. *Lagena*—an overlooked Oomycete genus with a wide range of hosts. *Mycological Progress* **21**(8): 66. doi: 10.1007/s11557-022-01818-9

Thines, M, Nam, B, Nigrelli, L, Beakes, G, Kraberg, A. 2015. The diatom parasite *Lagenisma coscinodisci* (Lagenismatales, Oomycota) is an early diverging lineage of the Saprolegniomycetes. *Mycological Progress* **14**(9): 75. doi: 10.1007/s11557-015-1099-y

Thingstad, TF. 2000. Elements of a theory for the mechanisms controlling abundance, diversity, and biogeochemical role of lytic bacterial viruses in aquatic systems. *Limnology and Oceanography* **45**(6): 1320–1328. doi: 10.4319/lo.2000.45.6.1320

Thompson, HF, Summers, S, Yuecel, R, Gutierrez, T. 2020. Hydrocarbon-degrading bacteria found tightly associated with the 50–70 µm cell-size population of eukaryotic phytoplankton in surface waters of a Northeast Atlantic region. *Microorganisms* **8**(12): 1955. doi: 10.3390/microorganisms8121955

Thomsen, HA, Buck, KR, Bolt, PA, Garrison, DL. 1991. Fine structure and biology of *Cryothecomonas* gen. nov. (protista incertae sedis) from the ice biota. *Canadian Journal of Zoology* **69**(4): 1048–1070. doi: 10.1139/z91-150

Tichy, L, Chytry, M. 2006. Statistical determination of diagnostic species for site groups of unequal size. *Journal of Vegetation Science* **17**(6): 809–818. doi: 10.1111/j.1654-1103.2006.tb02504.x

Tillmann, U, Hesse, K-J, Tillmann, A. 1999. Large-scale parasitic infection of diatoms in the Northfrisian Wadden Sea. *Journal of Sea Research* **42**(3): 255–261. doi: 10.1016/S1385-1101(99)00029-5

Underwood, GJC, Michel, C, Meisterhans, G, Niemi, A, Belzile, C, Witt, M, Dumbrell, AJ, Koch, BP. 2019. Organic matter from Arctic sea-ice loss alters bacterial community structure and function. *Nature Climate Change* **9**(2): 170–176. doi: 10.1038/s41558-018-0391-7

Veyssière, G, Castellani, G, Wilkinson, J, Karcher, M, Hayward, A, Stroeve, JC, Nicolaus, M, Kim, J-H, Yang, E-J, Valcic, L, Kauker, F, Khan, AL, Rogers, I, Jung, J. 2022. Under-ice light field in the western Arctic ocean during late summer. *Frontiers in Earth Science* **9**(February): 1–19. doi: 10.3389/feart.2021.643737

Walker, AM, Leigh, MB, Mincks, SL. 2023. Benthic bacteria and archaea in the North American Arctic reflect food supply regimes and impacts of coastal and riverine inputs. *Deep Sea Research Part II: Topical Studies in Oceanography* **207**(November 2022): 105224. doi: 10.1016/j.dsr2.2022.105224

Walsh, JE, Eicken, H, Redilla, K, Johnson, M. 2022. Sea ice breakup and freeze-up indicators for users of the Arctic coastal environment. *The Cryosphere* **16**(11): 4617–4635. doi: 10.5194/tc-16-4617-2022

Webster, MA, Rigor, IG, Nghiem, S V., Kurtz, NT, Farrell, SL, Perovich, DK, Sturm, M. 2014. Interdecadal changes in snow depth on Arctic sea ice. *Journal of Geophysical Research: Oceans* **119**(8): 5395–5406. doi: 10.1002/2014jc009985

Whitmore, L, Oggier, M, Dilliplaine, K, Kaufman, M, Bolt, C, Aguilar-Islas, A. 2024. Sea ice biogeochemistry time series at Utqiaġvik, Alaska (April - June 2021). Arctic Data Center. doi: 10.18739/A21J9793S

Yakimov, MM, Giuliano, L, Gentile, G, Crisafi, E, Chernikova, TN, Abraham, W-R, Lünsdorf, H, Timmis, KN, Golyshin, PN. 2003. *Oleispira antarctica* gen. nov., sp. nov., a novel hydrocarbonoclastic marine bacterium isolated from Antarctic coastal sea water. *International Journal of Systematic and Evolutionary Microbiology* **53**(3): 779–785. doi: 10.1099/ijs.0.02366-0

Yan, D, Yoshida, K, Nishioka, J, Ito, M, Toyota, T, Suzuki, K. 2020. Response to sea ice melt indicates high seeding potential of the ice diatom *Thalassiosira* to spring phytoplankton blooms: a laboratory study on an ice algal community from the Sea of Okhotsk. *Frontiers in Marine Science* **7**(July). doi: 10.3389/fmars.2020.00613

Yang, T, Nigro, LM, Gutierrez, T, D'Ambrosio, L, Joye, SB, Highsmith, R, Teske, A. 2016.

Pulsed blooms and persistent oil-degrading bacterial populations in the water column during and after the Deepwater Horizon blowout. *Deep Sea Research Part II: Topical Studies in Oceanography* **129**: 282–291. doi: 10.1016/j.dsr2.2014.01.014

Zhang, H, Wang, K, Shen, L, Chen, H, Hou, F, Zhou, X, Zhang, D, Zhu, X. 2018. Microbial community dynamics and assembly follow trajectories of an early-spring diatom bloom in a semienclosed bay. Kelly RM, editor. *Applied and Environmental Microbiology* **84**(18). doi: 10.1128/AEM.01000-18

Zhou, J, Richlen, ML, Sehein, TR, Kulis, DM, Anderson, DM, Cai, Z. 2018. Microbial community structure and associations during a marine dinoflagellate bloom. *Frontiers in Microbiology* **9**(JUN): 1–21. doi: 10.3389/fmicb.2018.01201

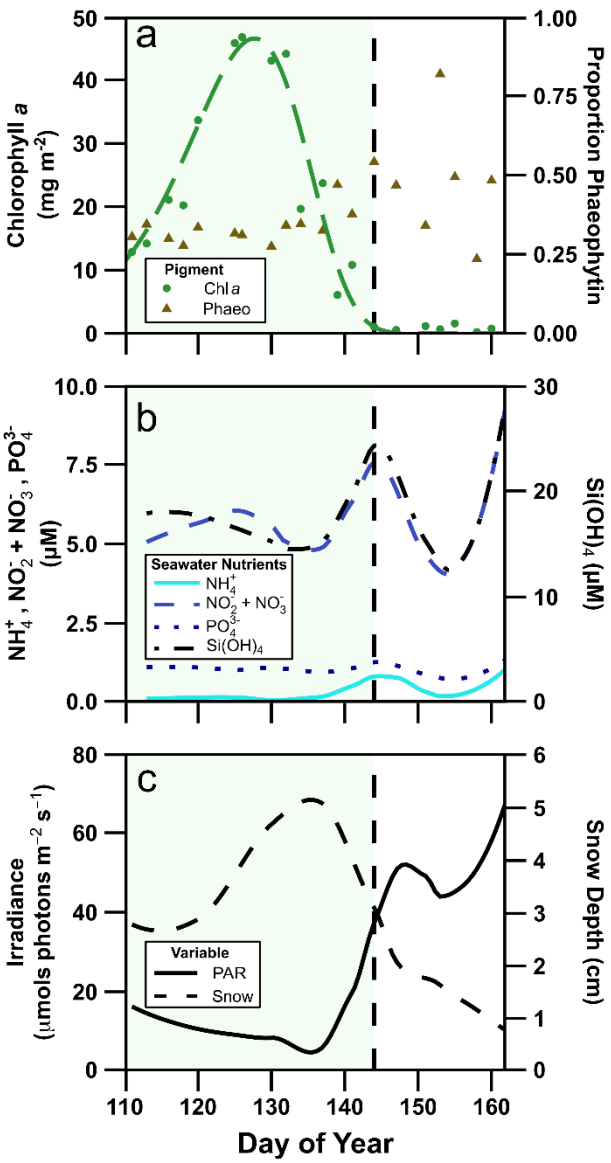

Figure 1. Development of biologically relevant measures over time. Temporal evolution of chlorophyll *a* and phaeophytin proportion (a), seawater concentrations of ammonium (NH_4^+), nitrite + nitrate (NO_2^- + NO_3^-), phosphate (PO_4^{3-}) and silicate ($Si(OH)_4$), (b), and snow thickness and under-ice PAR as measured by a spherical quantum sensor (4π; c). Green shading indicates the ice-algal bloom and the vertical dashed line indicates the bloom termination (<1 mg chlorophyll *a* m^{-2}).

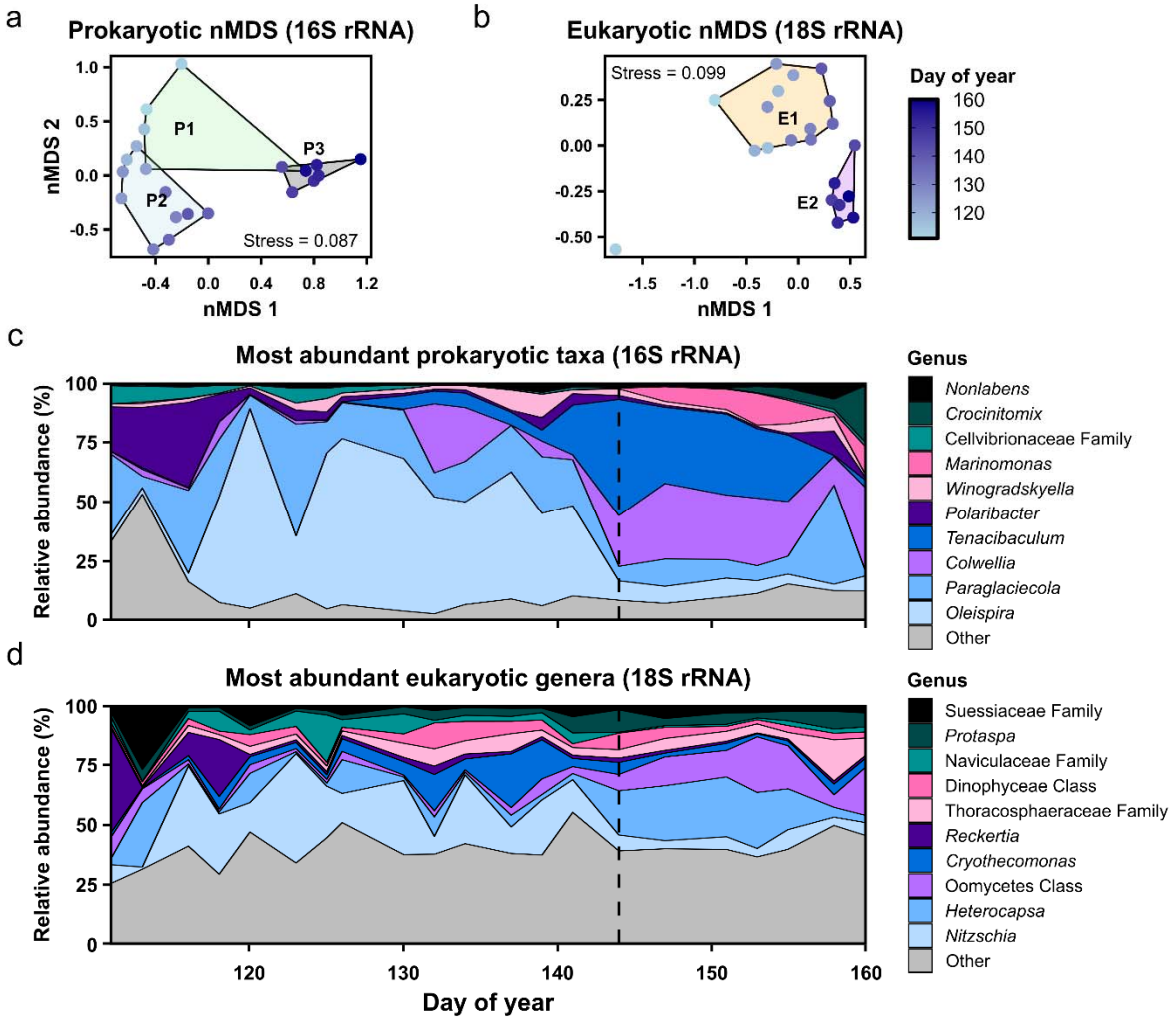

Figure 2. Sympagic microbial community structure and the most abundant genera over time. Non-metric multidimensional scaling (nMDS) ordination using Bray-Curtis dissimilarities (a & b). Sample groupings were determined by hierarchical clustering and labeled by their relation to the stage of the bloom. For prokaryotes (a), early- (P1), mid- (P2), and post-bloom (P3) clusters are observed. For Eukaryotes (b), bloom (E1) and post-bloom (E2) clusters were distinguished. Relative read contribution of the top 10 most abundant genera of prokaryotes (c) and unicellular eukaryotes (d). Vertical dashed line indicates bloom termination (<1 mg chlorophyll *a* m^{-2}).

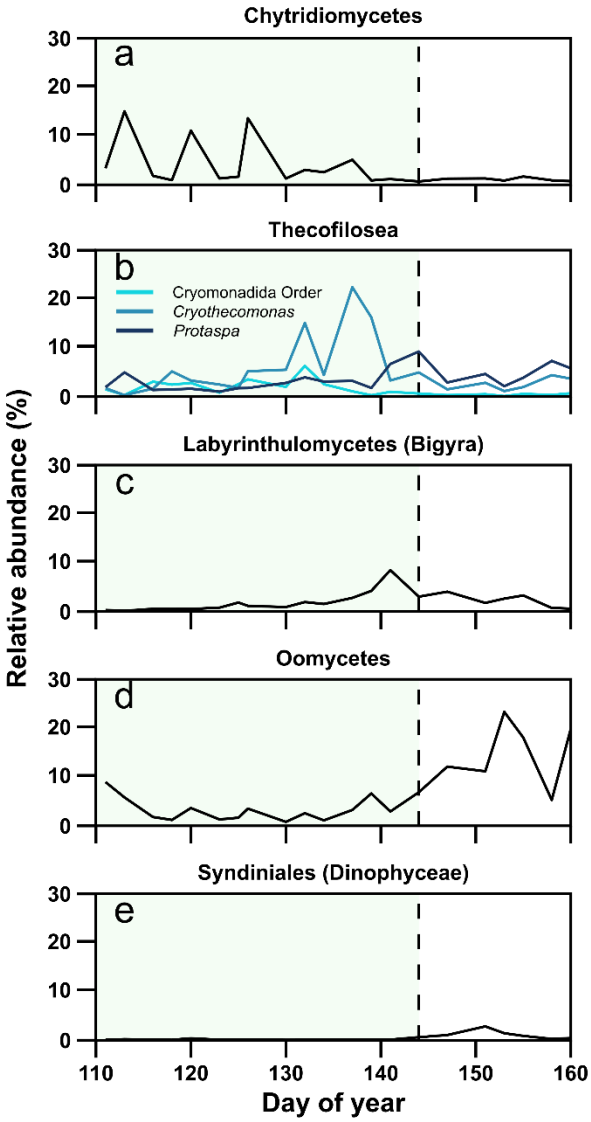

927

928 **Figure 3. Relative abundance of putative parasitoid groups over time.** (a) Chytridiomycota, class
929 Chytridiomycetes, (b) Cercozoa, class Thecofilosea, (c) Bigyra, order Labyrinthulomycetes, (d) Oomycetes,
930 (e) Dinoflagellata order Syndiniales. Green shading indicates the ice-algal bloom and the vertical dashed
931 line indicates the bloom termination (1 mg chlorophyll *a* m^{-2}).

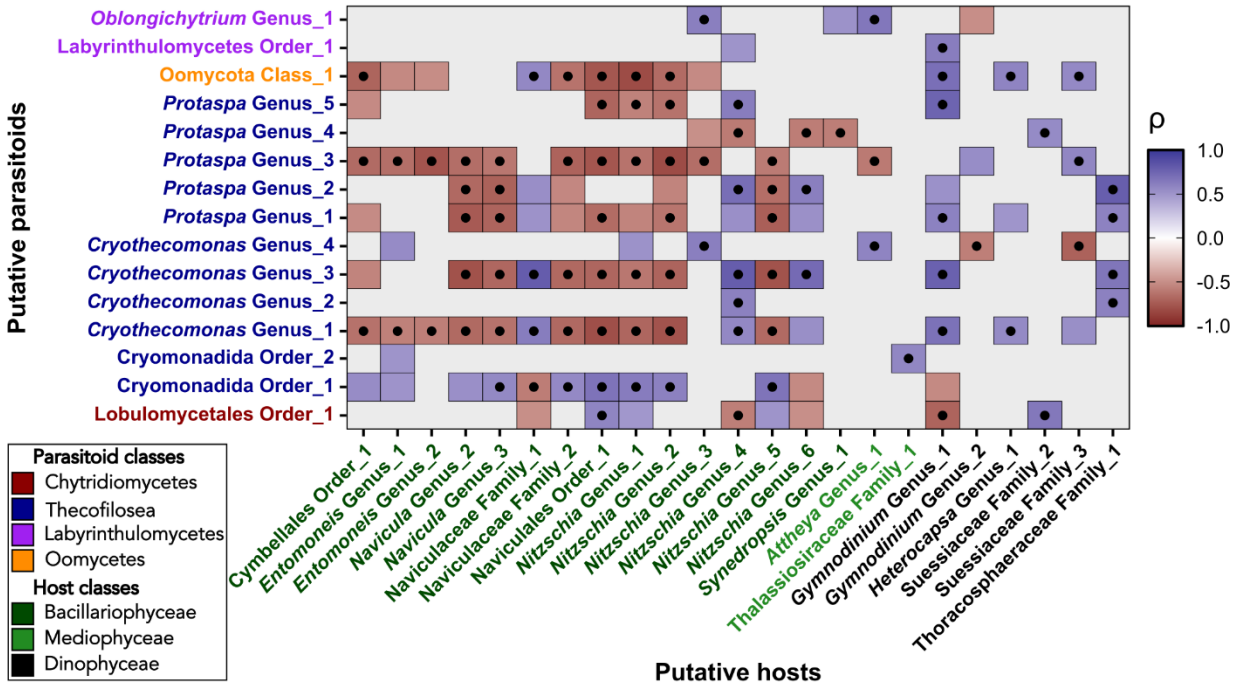

Figure 4. Correlation of putative parasitoids with putative hosts. Directed spearman correlation coefficient grid of amplicon sequence variants (ASVs) containing correlations between putative parasitoids and putative hosts with |rho| ≥ 0.5. Black dots indicate significant correlation (adj. $p < 0.05$).

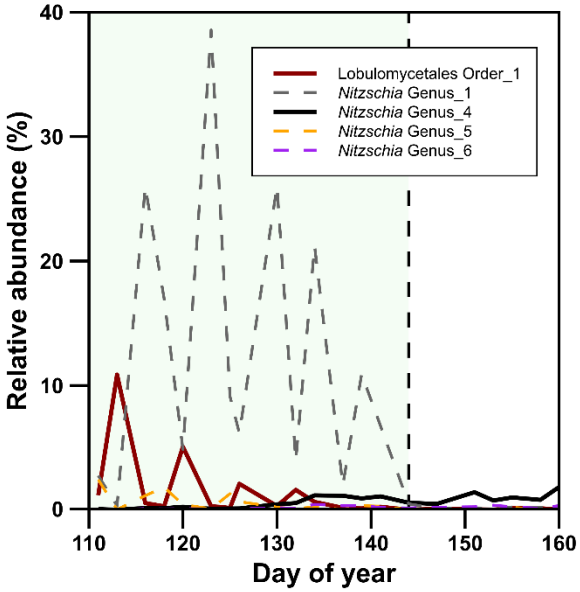

Figure 5. Relative abundance over time of a putative parasitoid (red line, Chytridiomycota) and *Nitzschia* hosts (black, grey, orange and purple lines). Solid lines indicate a significant correlation ($p < 0.05$); all *Nitzschia* ASVs presented here had a correlation coefficient ≥ |0.5|. Green shading indicates the ice-algal bloom and the vertical dashed line indicates the bloom termination (1 mg chlorophyll *a* m^{-2}).

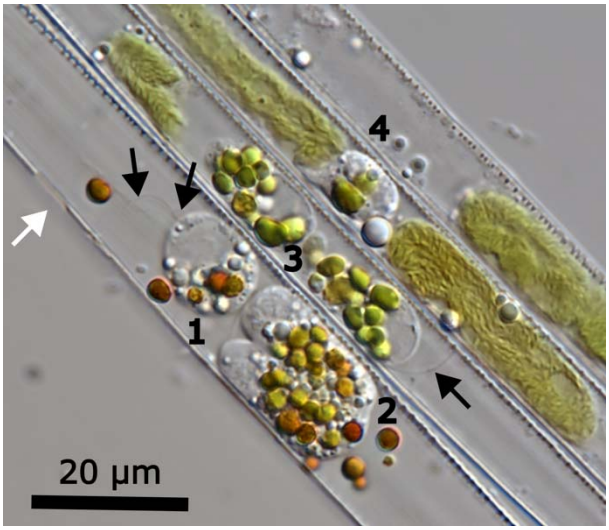

Figure 6. A small chain of *Nitzschia sp.* infected by *Cryothecomonas sp.* at different stages of infection, progressing from the bottom left to the top right. White arrow points to a compromise in the frustule that may be an entry point for the flagellate and black arrows point to flagella. 1) A mature flagellate with brown digestive vacuoles and surrounded by several defecated brown fecal bodies. 2) A large flagellate with many brown digestive vacuoles (the missing diatom plastids) with a cleavage furrow developing at the top left indicating the initiation of mitotic division. 3) Two small daughter cells with digestive vacuoles with fresh, still green, plastid material. Note the partially consumed plastid in the top left of the diatom frustule. 4) A single flagellate beginning to phagocytize the plastid of a newly infected diatom.